ESANN'1999 proceedings - European Symposium on Artificial Neural Networks
Bruges (Belgium), 21-23 April 1999, D-Facto public., ISBN 2-600049-9-X, pp. 1-6

Neural Field Description of State-Dependent Receptive Field Changes in the Visual Cortex

Katrin Suder*, Florentin Wörgötter*, and Thomas Wennekers†

*Institute of Physiology, Dept. of Neurophysiology,
Ruhr-University, 44780 Bochum, Germany
†Dept. of Neural Information Processing
University of Ulm, 89069 Ulm, Germany

Abstract. Receptive fields in V1 have been shown to be wider during synchronized than during non-synchronized EEG states, where, in addition, they can shrink over time in response to flashed stimuli. In the present paper we employ a neural field approach to describe the activity patterns in V1 analytically. Expressions for spatio-temporal receptive fields are derived and fitted to experimental data. The model supports the idea that the observed RF-restructuring is mainly driven by state-dependent LGN firing patterns (burst vs. tonic mode).

1. Introduction

Receptive field sizes in the primary visual cortex (V1) have recently been shown to depend on the state of the EEG [8]. In synchronized states (dominated by $\alpha-$ or $\delta-$waves) they are significantly wider than in less or non-synchronized states ($\beta-$EEG). In addition, in non-synchronized states their width can considerably shrink over time in response to flashed light spots (cf. Fig.1C and [8]). Different firing patterns of LGN during different EEG states have been suggested as the main mechanism for this restructuring [8]. During synchronized EEG, LGN cells respond to visual stimuli mainly with a contrast independent phasic burst of spikes at high frequency (Fig.1A). These bursts are strong enough to drive cortical cells also further away from the main projection column, whereby they evoke wide receptive fields. In contrast, during non-synchronized states, the burst component is often diminished. Instead, LGN cells respond with a long-lasting tonic firing pattern at much lower (and contrast dependent) rates (Fig.1B). Accordingly, one expects a transient and relatively broad initial receptive field (due to the burst) which sharpens quickly (due to the tonic component) just as observed experimentally (Fig.1C).

[0]Acknowledgements: K.S. and F.W. acknowledge the support of the DFG and of the HFSP. T.W. was supported by DFG grant Pa 268/8-1. The authors would like to thank K. Funke (Bochum) and H.E. Plesser (Göttingen) for valuable comments and discussions.

ESANN'1999 proceedings - European Symposium on Artificial Neural Networks
Bruges (Belgium), 21-23 April 1999, D-Facto public., ISBN 2-600049-9-X, pp. 1-6

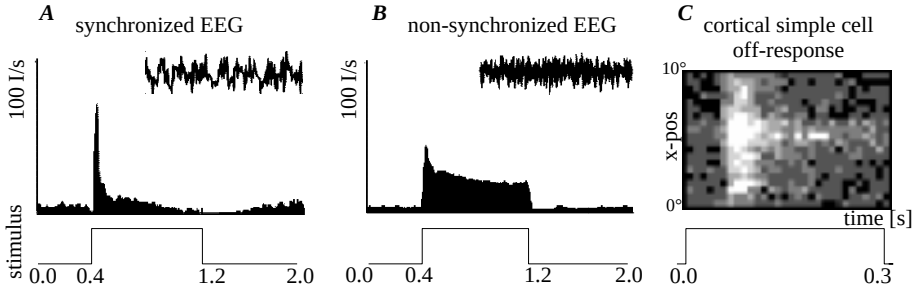

Fig.1: A,B: Peri-stimulus-time histograms of visual responses of a dLGN relay cell during different EEG states in an anesthetized cat. Note that in both EEG states, the neural response starts with bursting. Parts (5 s) from EEG-traces are shown in the insets. C: Shrinking of receptive field width of cortical cell with latency after stimulation. The total number of spikes is grey-scale coded (0-40 I/s).

The above hypothesis has been tested by means of biologically detailed computer simulations [8]. The present paper takes a more abstract level of description in form of neural field equations [1, 5, 7]. Those enable an analytical derivation of the spatio-temporal cortical activity. Moreover, cortical parameter sets can be obtained by fitting the model to experimental data.

2. Theory

The cortical layer V1 is idealized by a one-dimensional array of cells [1, 4, 5, 7]. V1 receives input from LGN whereas lateral and feedback connections are neglected. Those had been implemented in our earlier large scale simulations [8], but their influence was not essential for the main mechanisms of state-dependent receptive field sharpening. Therefore, the neural activity in V1, ϕ, can be written as a spatio-temporal convolution with the LGN input, $I(x,t)$:

$$\phi(x,t) = \int_0^t \int_{-\infty}^{\infty} g(t-t')K(x-x')I(x',t')dx'dt' \ . \qquad (1)$$

The kernel $g(t)$ in (1) describes the cortical temporal response function and $K(x)$ the feedforward projections from LGN to cortex. We choose

$$g(t) = \frac{1}{\tau}\, e^{-t/\tau} \quad \text{and} \quad K(x) = \frac{K_0}{\sqrt{2\pi}}\, e^{-\frac{x^2}{2\sigma_0^2}} \ . \qquad (2)$$

Thus, the temporal cortical dynamics is assumed to follow a first order low pass dynamics with empricical time-constant τ. In assuming a Gaussian connectivity profile for $K(x)$ we restrict our considerations to single on- or off-subfields. Receptive fields consisting of several subfields can be modeled by superpositions of several responses of the form (1) with appropriate g and K. The factor $K_0/\sqrt{2\pi}$ in (2) plays the role of an effective synaptic strength.

ESANN'1999 proceedings - European Symposium on Artificial Neural Networks
Bruges (Belgium), 21-23 April 1999, D-Facto public., ISBN 2-600049-9-X, pp. 1-6

In a first approximation, we assume that the input from LGN to V1 is separable in space and time: $I(x,t) = I_x(x)I_t(t)$ (cf.[3, 5]). Experimental stimuli in [8] are small light spots. Those evoke localized activity profiles in the LGN represented by a Gaussian function $I_x(x) = exp(-\frac{x^2}{2\sigma_1^2})$. The temporal component $I_t(t)$ of the LGN activity is modeled by phenomenological activity functions (3) and (4), which already contain the state-dependence and approximate the experimentally observed LGN firing patterns (Fig. 1):

$$Is_t(t) = c_1\Theta(t)\Theta(t_1 - t) \quad (3)$$

$$Ins_t(t) = Is_t(t) + c_2\Theta(t - t_1)\Theta(t_2 - t)\ . \quad (4)$$

$\Theta(t)$ is the Heaviside function. $Is_t(t)$ describes the high-frequency burst of spikes in the synchronized EEG in form of a rectangular pulse of strength c_1 lasting from $t = 0$ to t_1. The bursts are due to intrinsic LGN membrane properties (low-threshold Ca-bursts) and the interplay with inhibitory PGN neurons, modelled in more detail in [8]. $Ins_t(t)$ contains the additional tonic component of height $c_2 < c_1$ lasting from t_1 to t_2.

We are now ready to compute the cortical spatio-temporal activity profile $\phi(x,t)$. Because we assumed stimulation by small light spots, this profile can be interpreted as the cortical point spread function or, in light of the linearity and spatial homogeneity of the model, as the spatio-temporal receptive field of our model cells. Inserting the assumptions (2) – (4) into (1), one observes that the cortical response separates into a spatial component $X(x)$ and a temporal component $T(t)$, that is $\phi(x,t) = X(x)T(t)$. $X(x)$ is a convolution of two Gaussians, the input distribution $I_x(x)$ and the feedforward kernel $K(x)$:

$$X(x) = \frac{K_0\sigma_0\sigma_1}{\sqrt{\sigma_0^2+\sigma_1^2}}\, e^{-\frac{x^2}{2(\sigma_0^2+\sigma_1^2)}} = \frac{K_0\sigma_0\sigma_1}{\sigma_r}\, e^{-\frac{x^2}{2\sigma_r^2}} \approx K_0\sigma_1\, e^{-\frac{x^2}{2\sigma_0^2}}\ , \quad (5)$$

where $\sigma_r^2 := \sigma_0^2 + \sigma_1^2$ and the approximation holds for small stimuli, $\sigma_1 \ll \sigma_0$.

For the temporal factor $T(t)$ one gets in the non-synchronized state (4)

$$T(t) = \begin{cases} c_1(1 - e^{-\frac{t}{\tau}}) & : \quad 0 \le t < t_1 \\ c_2 - c_1e^{-\frac{t}{\tau}} + (c_1 - c_2)e^{-\frac{(t-t_1)}{\tau}} & : \quad t_1 \le t < t_2 \\ c_2e^{-\frac{(t-t_2)}{\tau}} - c_1e^{-\frac{t}{\tau}} + (c_1 - c_2)e^{-\frac{(t-t_1)}{\tau}} & : \quad t_2 \le t \end{cases} \quad (6)$$

The synchronized response $T(t)$ is obtained from (6) by setting $c_2 = 0$. A typical cortical response $\phi(x,t) = X(x)T(t)$ is shown in Fig. 2 (left).

From $\phi(x,t)$ we now derive lines of equal potential defined by

$$\phi(x,t) = X(x)T(t) = \kappa = const\ . \quad (7)$$

This relation can either be solved for $x = x(t;\kappa)$ or $t = t(x;\kappa)$ giving the equipotential lines in parameterized form. Of particular interest is the case where κ equals the firing threshold ϑ (which is assumed to be the same for all cells). Then $x(t;\kappa)$ describes the time course of the boundary between

ESANN'1999 proceedings - European Symposium on Artificial Neural Networks
Bruges (Belgium), 21-23 April 1999, D-Facto public., ISBN 2-600049-9-X, pp. 1-6

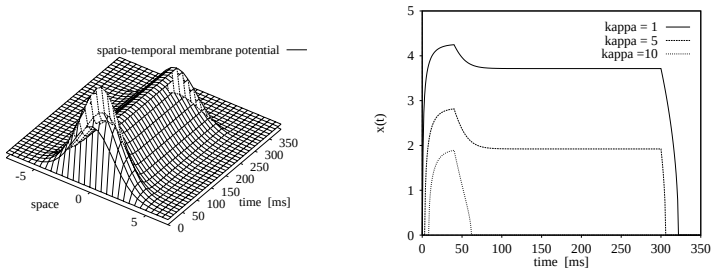

Fig.2: Left: $\phi(x,t)$ for the non-synchronized case with the following parameters: $\sigma_0 = 1.7, \sigma_1 = 0.5, \tau = 10.0ms$, $t_1 = 40ms$, $t_2 = 300ms$, $c_1 = 80I/s$, $c_2 = 40I/s$ (cf. Fig. 1 C). Right: $x(t)$ for different values of κ.

silent (subthreshold) and firing (superthreshold) cells. This is equivalent to the width of the spatio-temporal receptive fields as observed in experiments by extracellular recordings. Inserting $X(x)$, (5), into (7) and isolating x we get

$$x^2(t) = 2\sigma_r^2 \ln\left[\frac{K_0\sigma_0\sigma_1}{\kappa\sigma_r}T(t)\right] \overset{\sigma_1 \ll \sigma_0}{\approx} 2\sigma_0^2 \ln\left[\frac{K_0\sigma_1}{\kappa}T(t)\right] \ . \tag{8}$$

Using (6) for $T(t)$ we obtain the receptive field width for flashed stimuli. Example curves are plotted in Fig. 2 (right). Note that the width of the excited region closely resembles the experimental results although the width σ_r of the distribution of potentials is constant over time. The receptive field sharpening is explained by a decreasing region of cells above threshold.

In a next step, $t(x)$ could be determined. For $\kappa = \vartheta$ this defines the times, when cells at location x reach threshold, i.e. when they start or stop firing.

3. Fit to Experimental Data

To test whether the model can accurately describe the experimental data and to estimate the model parameters, we fitted recorded firing rates $\nu(x,t)$ of on- and corresponding off-subfields of 16 V1 cells during epochs of both EEG states. Each field was sampled at 20 positions with .5 degree resolution and for 30 time slices of 10 ms bin size (cf. Fig. 1C). The potentials $\phi(x,t)$ are supposed to transform into firing rates by means of a rectilinear function $f(\phi) = \beta[\phi - \vartheta]_+ + b$ where b accounts for spontaneous background firing. Note, that $\phi(x,t)$ contains products of model parameters (see Eqn.s 5 and 6). This implies that we cannot determine all these parameters independently. For the same reason we may set β to unity. We first determined the parameters of $X(x)$ by nonlinear least square fits (Levenberg-Marquardt) of every time slice t_i of the data to the function

$$\nu(x,t_i) \overset{fit}{=} \left[qe^{-\frac{(x-a)^2}{2\sigma_r^2}} - \vartheta\right]_+ + b \ . \tag{9}$$

Here, a is an (arbitrary) offset of the receptive field center and $q(t_i)$ is proportional to $T(t_i)$ (see below). It turned out that the parameters $\sigma_r(t_i), a(t_i), b(t_i)$,

ESANN'1999 proceedings - European Symposium on Artificial Neural Networks
Bruges (Belgium), 21-23 April 1999, D-Facto public., ISBN 2-600049-9-X, pp. 1-6

$\vartheta(t_i)$ obtained this way were almost constant over time as can be seen in Fig.s 3A,B (mean (all data sets) standard deviations: a: 6%, σ_r: 28%, b: 23%, ϑ: 17%). This justifies our approach: the fact, that the width of the spatial activity profile σ_r is constant over time (Fig. 3A) supports the hypothesis that the restructuring is not due to recurrent connections in V1. Those would also sharpen ϕ (see [6]). The time courses of the parameters did not show systematic trends with the exception of b: the fitted background was slightly larger during the initial part of the response driven by the LGN-bursts (Fig. 3B).

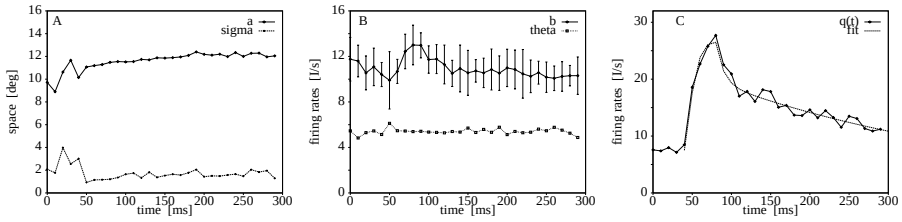

Fig.3: Time course of model parameters for an example data set. A: Position of the center of the Gaussian a and the width σ_r. B: Firing threshold ϑ and background activity b (with standard deviation). C: $q(t)$ and the nonlinear fit. Note that the LGN activity does not reach V1 before a delay of approx. 40 ms.

In a second step we fitted $q(t_i)$ to $kT(t-t_0)$ with $k = K_0\sigma_0\sigma_1/\sigma_r$ (Eqn. (5)) to determine the temporal parameters $C_1 := kc_1, C_2 := kc_2, t_0, t_1, t_2$, and τ. Again, only products kc_i can be obtained from the fit. t_0 accounts for latencies between stimulus onset and cortical response, which are not contained in our model. t_2 was fixed at 300 ms because data were only sampled during stimulus presentation. For most subfields good fits were obtained (cf. Fig. 3C). The on-subfields in the non-synchronized case exhibited a significant adaptation during the tonic phase (cf. Fig. 3C, 100–300 ms). In these cases adaptation was added, i.e. c_2 was replaced by $c_2 exp(-(t-t_1)/\tau_a)$.

The fits revealed that the main difference between on- and off-subfields is a delay of the off-fields of 10-20 ms, which is in accordance with the literature. The main EEG state-dependence turns out to be the difference between C_1 and C_2, which are proportional to the LGN activity during burst and tonic phase. It is about twice as high in the synchronized (51 I/s) than in the non-synchronized state (25 I/s). Moreover, we find that bursts are more pronounced (88±5 vs. 70±4 I/s) and the tonic component is smaller (36±2 vs. 45±3 I/s) during synchronized EEG. The other model parameters do not exhibit dependences on the EEG-state or on subfield types. Standard deviations for the temporal model parameters are very small (1-10%), i.e. the dynamics is well covered by the simple model. Somewhat surprisingly, even the empirical time-constant τ appeared to be the same in the different EEG states. Since neuronal membranes tend to have faster response-times in the depolarized states one may have expected differences in τ. The lack is not completely clear; the experiments might have been performed in a range of depolarization where τ is almost constant. In agreement with the literature [3, 6], we find the following mean values: $\tau = 13 \pm 7$ ms, $t_1 - t_0 = 38 \pm 17$ ms, $\tau_a = 541 \pm 238$ ms.

ESANN'1999 proceedings - European Symposium on Artificial Neural Networks
Bruges (Belgium), 21-23 April 1999, D-Facto public., ISBN 2-600049-9-X, pp. 1-6

4. Conclusions

We have introduced a neural field model of LGN and V1 to describe EEG-dependent receptive field changes in V1 [8]. The analytic expressions for the cortical spatio-temporal activity, Eqns. (5) and (6), show that the restructuring can be explained by state-dependent thalamic firing patterns (burst vs. tonic mode) and a pure feedforward mechanism. To test this hypothesis the model was fitted to experimental data. Here, it is most important that the width σ_r of the spatial profile of the estimated membrane potentials ϕ and the firing thresholds ϑ of cells remain constant over time during a whole response period, even though a strong modulation of the receptive field is present (as measured from spike rates). This supports the hypothesis that the experimentally observed receptive field changes are mainly due to input from LGN and not so much due to recurrent synaptic interactions in V1. Such intracortical circuits have been suggested to be responsible for the sharpening of orientation tuning curves [2, 6]. In contrast to our model, recurrent processes would lead to changes in the width σ_r, which was not confirmed by the results of the fit.

References

[1] S.I. Amari. Dynamics of pattern formation in lateral-inhibition type neural fields. *Biol. Cybernetics*, 27:77–87, 1977.

[2] R. Ben-Yishai, R.L. Bar-Or, and H. Sompolinsky. Theory of orientation tuning in visual cortex. *Proc Natl Acad Sci U S A*, 92:3844–8, 1995.

[3] G.C. DeAngelis, I. Ohzawa, and R.D. Freeman. Receptive-field dynamics in the central visual pathway. *TINS*, 18:451–458, 1995.

[4] G. Krone, H. Mallot, G. Palm, and A. Schüz. Spatiotemporal receptive fields: a dynamical model derived from cortical architectonics. *Proc. R. Soc. Lond.*, 226:421–444, 1986.

[5] P. Mineiro and D. Zipser. Analysis of direction selectivity arising from recurrent cortical interactions. *Neural Computation*, 10:353–371, 1998.

[6] D.C. Somers, S.B. Nelson, and M. Sur. An emergent model of orientation selectivity in cat visual cortical simple cells. *J. Neurosci.*, 15:5465–88, 1995.

[7] H.R. Wilson and J.D. Cowan. A mathematical theory of the functional dynamics of cortical and thalamic nervous tissue. *Kybernetik*, 13:55–80, 1973.

[8] F. Wörgötter, K. Suder, Y. Zhao, N. Kerscher, U. Eysel, and K. Funke. State-dependent receptive field restructuring in the visual cortex. *Nature*, 396(6707):165–168, 1998.